*Int. J. Electrochem. Sci.*, 4 **(2009)** 1568 - 1582

**International Journal of ELECTROCHEMICAL SCIENCE**
www.electrochemsci.org

# Aplication of Phenolic Acids in the Corrosion Protection of Al-0.8Mg Alloy in Chloride Solution

*L. Vrsalović*[*]*, M. Kliškić and S. Gudić*

Department of Electrochemistry and Protection of Materials, Faculty of Chemistry and Technology, University of Split, Teslina 10/V, 21000 Split, Croatia
[*]E-mail: ladislav@ktf-split.hr

*Received:* 28 October 2009 / *Accepted:* 11 November 2009 / *Published:* 1 December 2009

The inhibiting action of sinapinic and gentisic acid on Al-0.8Mg alloy in 0.5 mol $dm^{-3}$ NaCl solution was studied using potentiodynamic polarization method, linear polarization method, and electrochemical impedance spectroscopy measurements. Investigations were performed on a rotating disc electrode in a quiescent solution and at different electrode rotation rates and electrolyte temperatures. The results indicate that the investigated phenolic acids act as cathodic corrosion inhibitors for the Al-0.8Mg alloy, and the inhibition efficiency increases with increasing inhibitor concentration but decreases with increasing electrode rotation rate and electrolyte temperature. A mechanism of physical adsorption is proposed for the inhibition behaviour and the adsorption characteristics of the inhibitors were approximated by Freundlich adsorption isotherm.

**Keywords:** Al-0.8Mg alloy, corrosion, electrochemical techniques, phenolic acids, Freundlich adsorption isotherm

## 1. INTRODUCTION

Aluminium and its alloys are important materials for use in many applications, such as for automobiles, aviation, household appliances, containers and electronic devices [1-3], owning to its many favourable characteristics - including low density, good electrical and thermal conductivities, high ductility and good corrosion resistance. The application of aluminium and its alloys are often possible because of the natural tendency of aluminium to form a passivating oxide layer. However, in aggressive media, the passivating layer can be destroyed, and corrosive attack can take place. The protection of aluminium and its oxide films against the corrosive action of chloride ions have been extensively investigated and a great number of inhibitors have been studied [4-10]. Unfortunately, many common corrosion inhibitors are health hazards, so researchers are focused in finding

environment friendly inhibitors [11-15]. Naturally occurring antioxidants are cheap, readily available and renewable sources of materials, and can be used as corrosion inhibitors. These organic compounds are either synthesised or either extracted from aromatic herbs, spices and medicinal plants [16-18].

This study was a continuation of the research of corrosion inhibition of Al-Mg alloys with compounds that exist in Mediterranean plant *Rosmarinus officinalis* L., The authors had previously found that neutral fraction of aqueous extract *Rosmarinus officinalis* L., with its dominant compound (+)-catechine, can served as adequate corrosion inhibitor of Al-2.5Mg alloy in sodium chloride solution [17,19]. Acidic subfractions of aqueous extract, which contained different phenolic acids, also have shown corrosion inhibition characteristics [20,21]. One of identified phenolic acid in acidic aqueous fraction of rosemary leaves was sinapinic acid and results of investigations with the pure sinapinic acid have shown that this acid act as cathodic corrosion inhibitor for Al-2.5Mg alloy [22].

In this paper we present the novel results of corrosion inhibition of Al-Mg alloy with phenolic acids. We used Al-0.8Mg alloy as a working material and two phenolic acids, sinapinic and gentisic acid, which was found in the acidic fraction of the aqueous extract of Rosemary leaves. The procedure of obtaining acidic fractions from the aqueous extract of Rosemary leaves has been described previously [19]. These phenolic acids show good antioxidant activity [23,24] and also antibacterial and weak anti-fungal activity [25,26].

## 2. EXPERIMENTAL PART

A disc-working electrode suitable for a Radiometer Analytical EDI 101 rotating disc system was machined from a cylindrical rod with a diameter of 8 mm. The chemical composition of the Al-0.8Mg alloy was Mg-0.8%, Fe-0.2%, Si-0.1% and Al-98.9%. The exposed electrode surface was abraded with different grades of emery papers, polished with alumina slurries (0.5 and 0.05 μm), degreased in ethanol, rinsed with doubly distilled water and left a few minutes in the air to form the "natural" oxide film before being immersed in the solution. Electrochemical experiments were carried out in a conventional three-electrode electrochemical cell, with a platinum counter electrode and a saturated calomel electrode (SCE), placed in Luggin capillary, as a reference electrode. All potentials are referred to a SCE electrode. Investigated solutions were prepared from p.a. reagents. The basic solution was 0.5 mol $dm^{-3}$ NaCl solution to which sinapinic acid was added in concentrations of $1\times10^{-6}$, $1\times10^{-5}$, $5\times10^{-5}$, $1\times10^{-4}$ and $5\times10^{-4}$ mol $dm^{-3}$, and gentisic acid in concentrations of $1\times10^{-5}$, $5\times10^{-5}$, $1\times10^{-4}$, $5\times10^{-4}$ and $1\times10^{-3}$ mol $dm^{-3}$. The chemical structures of the investigated compounds are given in Fig. 1.

The pH values of all investigated solutions were adjusted to 6 using sodium hydroxide solution. The experiments were performed in a quiescent solution in the temperature range from 20 °C to 50 °C, and at the electrode rotation rates 150 rpm and 2000 rpm.

Potentiodynamic polarization measurements were performed with the scan rate of 0.2 mV $s^{-1}$ in potential range of –200 mV to +150 mV from corrosion potential ($E_{corr}$), and in potential range ±10 mV around $E_{corr}$ for polarization resistance measurements. Impedance measurements were performed in quiescent solution at $E_{corr}$ with the a.c. amplitude ±10 mV in the frequency range from 50 kHz to

30 mHz. Polarization and impedance measurements were carried out by a PAR EG&G potentiostat/galvanostat (Model 273A) and a PAR EG&G lock-in amplifier (Model 5210).

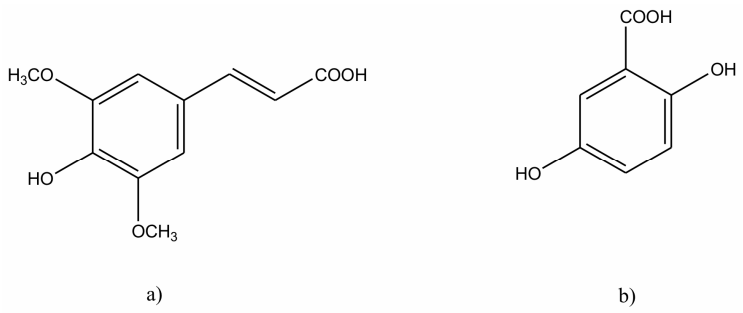


**Figure 1.** Chemical structure of sinapinic acid a) and gentisic acid b).

## 3. RESULTS AND DISCUSSION

### *3.1. Polarization measurements*

Typical potentiodynamic polarization curves for Al-0.8Mg alloy in a 0.5 mol $dm^{-3}$ NaCl solution in the absence and presence of different concentrations of sinapinic and gentisic acid at 20 °C, are shown in Figs. 2-3.

Changes observed in the polarization curves after addition of the inhibitors are usually used as the criteria to classify inhibitors as cathodic, anodic or mixed [27]. In our case, the modifications caused by addition of sinapinic and gentisic acid to the NaCl solution are a negative shift on the corrosion potential and a leftward displacement in the cathodic branch of the curves. In the anodic domain the i-E characteristics remained almost the same. Taking into account all polarization characteristics it can be concluded that sinapinic and gentisic acid can be classified as cathodic-type inhibitors.

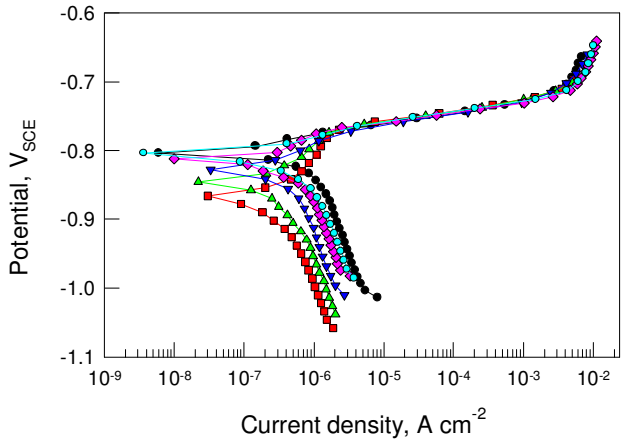


**Figure 2.** Potentiodynamic polarization curves for the Al-0.8Mg alloy in quiescent 0.5 mol $dm^{-3}$ NaCl solution at 20°C without (●) and in the presence of sinapinic acid in the concentration of $1\times10^{-6}$ (●), $1\times10^{-5}$ (♦), $5\times10^{-5}$ (▼), $1\times10^{-4}$ (▲) and $5\times10^{-4}$ mol $dm^{-3}$ (■).

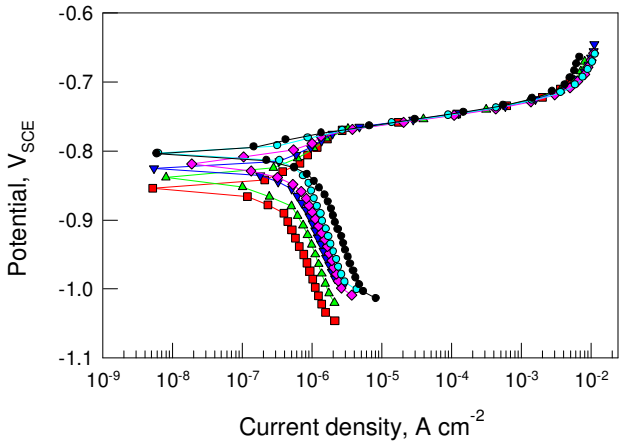


**Figure 3.** Potentiodynamic polarization curves for the Al-0.8Mg alloy in quiescent 0.5 mol $dm^{-3}$ NaCl solution at 20°C without (●) and in the presence of gentisic acid in the concentration of $1\times10^{-5}$ (●), $5\times10^{-5}$ (♦), $1\times10^{-4}$ (▼), $5\times10^{-4}$ (▲) and $1\times10^{-3}$ mol $dm^{-3}$ (■).

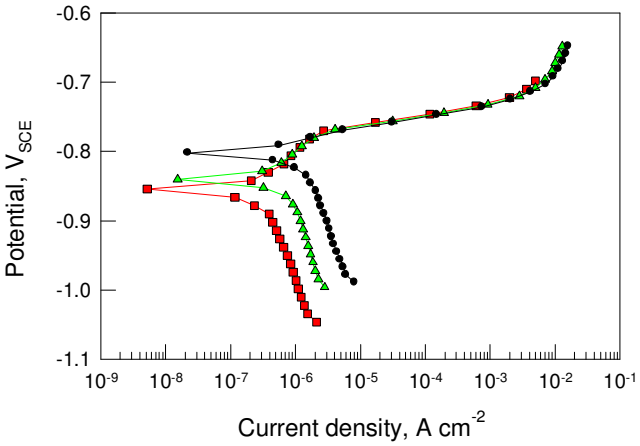


**Figure 4.** Potentiodynamic polarization curves for the Al–2.5Mg alloy in 0.5 mol $dm^{-3}$ NaCl solution in the presence of gentisic acid in the concentration of $1\times10^{-3}$ mol $dm^{-3}$, at 20 C and different electrode rotation rates: ω = 0 rpm (■), ω = 150 rpm (▲) and ω = 2000 rpm (●).

The influence of electrode rotation rate on potentiodinamic polarization curves is shown in Fig. 4.

From the Fig. 4 it can be seen that increasing the electrode rotation rate leads to increase in cathodic current density and to shifting the corrosion potential to positive values, which indicates the weakening of the inhibitive action of gentisic acid. The similar results have been obtained in measurements with sinapinic acid.

Table 1 shows the electrochemical polarization parameters for the investigated alloy in a NaCl solution without and in the presence of different concentrations of investigated phenolic acids at different electrode rotation rates. The parameters include the corrosion potential ($E_{corr}$), the corrosion

current density ($i_{corr}$), the percentage of inhibition efficiency (η), and surface coverage (Θ). The percentage of inhibition efficiency and surface coverage was calculated using equations (1) and (2):

$$\Theta = \frac{i_{corr} - (i_{corr})_i}{i_{corr}} \quad (1)$$

$$\eta = \frac{i_{corr} - (i_{corr})_i}{i_{corr}} \times 100 \quad (2)$$

where $i_{corr}$ and $(i_{corr})_i$ are corrosion current densities in the absence and presence of inhibitor.

**Table 1.** Corrosion current density, corrosion potential, surface coverage and inhibition efficiency for the Al-0.8Mg alloy in 0.5 mol $dm^{-3}$ NaCl solution with addition of different concentration of sinapinic and gentisic acid

| | | sinapinic acid | | | | gentisic acid | | | |
|---|---|---|---|---|---|---|---|---|---|
| c (inhibitor) (mol $dm^{-3}$) | ω (rpm) | $E_{corr}$ (V) | $i_{corr}$ (μA $cm^{-2}$) | Θ | η (%) | $E_{corr}$ (V) | $i_{corr}$ (μA $cm^{-2}$) | Θ | η (%) |
| 0 | 0 | -0.805 | 0.90 | - | - | -0.805 | 0.90 | - | - |
| $1\times10^{-6}$ | | -0.804 | 0.57 | 0.3666 | 36.66 | - | - | - | - |
| $1\times10^{-5}$ | | -0.812 | 0.48 | 0.4667 | 46.67 | -0.803 | 0.59 | 0.3444 | 34.44 |
| $5\times10^{-5}$ | | -0.828 | 0.41 | 0.5444 | 54.44 | -0.818 | 0.53 | 0.4111 | 41.11 |
| $1\times10^{-4}$ | | -0.840 | 0.35 | 0.6111 | 61.11 | -0.821 | 0.47 | 0.4778 | 47.78 |
| $5\times10^{-4}$ | | -0.859 | 0.29 | 0.6778 | 67.78 | -0.838 | 0.40 | 0.5556 | 55.56 |
| $1\times10^{-3}$ | | | - | - | - | -0.855 | 0.35 | 0.6111 | 61.11 |
| 0 | 150 | -0.793 | 1.32 | - | - | -0.793 | | | |
| $1\times10^{-6}$ | | -0.783 | 0.96 | 0.2727 | 27.27 | - | - | - | - |
| $1\times10^{-5}$ | | -0.785 | 0.82 | 0.3788 | 37.88 | -0.781 | 0.97 | 0.2651 | 26.51 |
| $5\times10^{-5}$ | | -0.800 | 0.74 | 0.4394 | 43.94 | -0.789 | 0.87 | 0.3409 | 34.09 |
| $1\times10^{-4}$ | | -0.821 | 0.66 | 0.5000 | 50.00 | -0.802 | 0.80 | 0.3939 | 39.39 |
| $5\times10^{-4}$ | | -0.834 | 0.55 | 0.5833 | 58.33 | -0.820 | 0.72 | 0.4545 | 45.45 |
| $1\times10^{-3}$ | | | - | - | - | -0.840 | 0.62 | 0.5303 | 53.03 |
| 0 | 2000 | -0.771 | 2.08 | - | - | -0.771 | 2.08 | - | - |
| $1\times10^{-6}$ | | -0.774 | 1.76 | 0.1538 | 15.38 | - | - | - | - |
| $1\times10^{-5}$ | | -0.780 | 1.55 | 0.2548 | 25.48 | -0.775 | 1.76 | 0.1538 | 15.38 |
| $5\times10^{-5}$ | | -0.784 | 1.44 | 0.3077 | 30.77 | -0.773 | 1.61 | 0.2259 | 22.59 |
| $1\times10^{-4}$ | | -0.795 | 1.35 | 0.3509 | 35.09 | -0.780 | 1.52 | 0.2692 | 26.92 |
| $5\times10^{-4}$ | | -0.807 | 1.19 | 0.4279 | 42.79 | -0.789 | 1.42 | 0.3173 | 31.73 |
| $1\times10^{-3}$ | | | - | - | - | -0.803 | 1.28 | 0.3846 | 38.46 |

The data from Table 1 shows that the increasing the phenolic acids concentration markedly decreases the corrosion current density and consequently increases the values of the surface coverage and the percentage inhibition. The efficiency of the phenolic acids decreases with increase in electrode rotation rate. Smaller values of corrosion current densities, obtained by the measurements with sinapinic acid, and higher values of surface coverage and inhibition efficiency indicate that the sinapinic acid is better corrosion inhibitor for Al-0.8Mg alloy than gentisic acid.

The similar polarization curves are obtained in measurements with Al-2.5Mg alloy 0.5 mol $dm^{-3}$ NaCl solution without and in the presence of different concentrations of sinapinic acid [22].

If we compare these results with the results of potentiodynamic polarization measurements with Al-2.5Mg alloy at the same experimental conditions, it can be seen that the values of corrosion current densities for Al-0.8Mg alloy are lower then the values of corrosion current densities for the Al-2.5Mg alloy. This can be explained by differences in composition of these two alloys. Al-2.5Mg alloy has higher amount of alloying elements, which improves mechanical properties of this alloy but probably is reducing its corrosion resistance. Added alloying elements can be present in aluminium alloy in the form of precipitates, inclusions and intermetallic compounds in different shapes, sizes and composition and represent an important factor of corrosion behaviour of aluminium alloys [28]. It is known that increasing the Mg content in Al-Mg alloys, significantly increases the strength of the alloys without substantial impact on formability [29,30]. However, increasing the magnesium content leads to increasing the so-called β-phase ($Al_3Mg_2$) content in the alloys, which usually precipitate at the grain boundaries or on the alloy surface. Present intermetallic particles like $Al_3Mg_2$ and $Mg_5Al_8$ are anodic, compared with the surrounded aluminium matrix, and represent the places where initial corrosion attack takes place [31,32]. As Al-2.5Mg alloy has higher Mg content, compared to Al-0.8Mg alloy, it can be expected that this alloy contains more intermetallic particles then Al-0.8Mg alloy, which could explain the results of polarization measurements for this two alloys.

The effect of temperature on the corrosion of Al-0.8Mg alloy and its inhibition with phenolic acids was studied in temperature range of 20 – 50 $^{o}$C. The results of investigations have shown that corrosion rate of Al-0.8Mg alloy in both free and inhibited NaCl solution increased as the temperature was increased. The dependence of the corrosion current on temperature can be regarded as an Arrhenius-type process, the rate of which is:

$$i_{corr} = A\exp\left(-\frac{E_a}{RT}\right) \qquad (3)$$

where $i_{corr}$ is the corrosion current density, A is the Arrhenius preexponential constant and $E_a$ is the apparent activation energy.

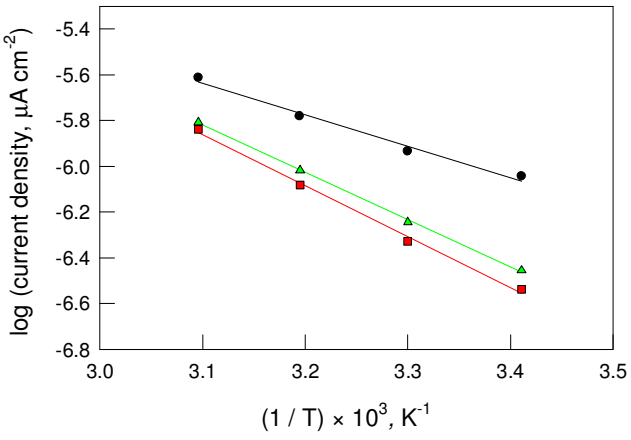


**Figure 5**. Activation energy determination for the Al-0.8Mg alloy in a 0.5 mol dm$^{-3}$ NaCl solution without (●) and in the presence of sinapinic acid in the concentration of 5×10$^{-4}$ mol dm$^{-3}$ (■), and gentisic acid in concentration of 1×10$^{-3}$ mol dm$^{-3}$ (▲).

Plotting log current density versus 1/T gives a straight line, as revealed by Fig. 5.

The values of activation energy determined from the slopes of these plots and calculated from the equation (3) are:

$E_{a1}$ = 26.36 kJ $mol^{-1}$ in a noninhibited 0.5 mol $dm^{-3}$ NaCl solution,
$E_{a2}$ = 42.68 kJ $mol^{-1}$ with the addition of $5\times10^{-4}$ mol $dm^{-3}$ sinapinic acid
$E_{a3}$ = 39.90 kJ $mol^{-1}$ with the addition of $1\times10^{-3}$ mol $dm^{-3}$ gentisic acid.

Generally, if the inhibitive additive cause a rise in activation energy value when compared to the base solution, that could be interpreted by physical adsorption [33,34]. Also physical adsorption is related to lower values of the activation energy (30 – 50 kJ $mol^{-1}$) [33], which is agreeable to the presented results.

**Table 2.** Polarization resistance, surface coverage and inhibition efficiency for the Al-0.8Mg alloy in a 0.5 mol $dm^{-3}$ NaCl solution without and with addition of different concentration of sinapinic and gentisic acid at 20 ºC and different electrode rotation rates

| | | sinapinic acid | | | gentisic acid | | |
|---|---|---|---|---|---|---|---|
| c (inhibitor) (mol $dm^{-3}$) | ω (rpm) | $R_p$ (kΩ $cm^2$) | Θ | η (%) | $R_p$ (kΩ $cm^2$) | Θ | η (%) |
| 0 | 0 | 8.128 | - | - | 8.128 | - | - |
| $1\times10^{-6}$ | | 12.052 | 0.3256 | 32.56 | - | - | - |
| $1\times10^{-5}$ | | 14.923 | 0.4553 | 45.53 | 11.892 | 0.3165 | 31.65 |
| $5\times10^{-5}$ | | 17.455 | 0.5343 | 53.43 | 13.133 | 0.3811 | 38.11 |
| $1\times10^{-4}$ | | 21.369 | 0.6196 | 61.96 | 15.255 | 0.4672 | 46.72 |
| $5\times10^{-4}$ | | 26.835 | 0.6971 | 69.71 | 17.924 | 0.5465 | 54.65 |
| $1\times10^{-3}$ | | - | - | - | 20.932 | 0.6117 | 61.17 |
| 0 | 150 | 6.997 | - | - | 6.997 | - | - |
| $1\times10^{-6}$ | | 9.263 | 0.2446 | 24.46 | - | - | - |
| $1\times10^{-5}$ | | 10.630 | 0.3418 | 34.18 | 9.092 | 0.2304 | 23.04 |
| $5\times10^{-5}$ | | 12.254 | 0.4290 | 42.90 | 9.932 | 0.2955 | 29.55 |
| $1\times10^{-4}$ | | 14.868 | 0.5294 | 52.94 | 11.693 | 0.4016 | 40.16 |
| $5\times10^{-4}$ | | 18.744 | 0.6267 | 62.67 | 13.228 | 0.4710 | 47.10 |
| $1\times10^{-3}$ | | - | - | - | 15.465 | 0.5476 | 54.76 |
| 0 | 2000 | 4.439 | - | - | 4.439 | - | - |
| $1\times10^{-6}$ | | 5.055 | 0.1219 | 12.19 | - | - | - |
| $1\times10^{-5}$ | | 5.594 | 0.2065 | 20.65 | 4.997 | 0.1117 | 11.17 |
| $5\times10^{-5}$ | | 6.236 | 0.2882 | 28.82 | 5.428 | 0.1822 | 18.22 |
| $1\times10^{-4}$ | | 7.222 | 0.3854 | 38.54 | 6.137 | 0.2767 | 27.67 |
| $5\times10^{-4}$ | | 8.308 | 0.4657 | 46.57 | 6.655 | 0.3330 | 33.30 |
| $1\times10^{-3}$ | | - | - | - | 7.646 | 0.4194 | 41.94 |

The polarization resistance measurements were performed by applying a controlled potential scan over a small range, ±10 mV with respect to $E_{corr}$. The resulting current is linearly plotted versus potential and the slope of this plot at $E_{corr}$ being the polarization resistance, $R_p$.

The $R_p$ values were used to calculate the inhibiting efficiency η, using the equation (4):

$$\eta = \left( \frac{R_{pi} - R_p}{R_{pi}} \right) \times 100 \quad (4)$$

where $R_p$ and $R_{pi}$ are the polarization resistances without and with the addition of inhibitor.

The values of the determined polarization resistance and the values of the inhibitor efficiency calculated using Equation 4 are shown in Table 2.

It can be seen that $R_p$ values increased with increasing the inhibitors concentration, but decreased with increase in electrode rotation rate end also with the increase of electrolyte temperature. The values of inhibitor efficiency, calculated from $R_p$ values, are in good agreement with the values calculated from corrosion current densities from potentiodynamic polarization measurements.

From the Table 2 it can be seen that the higher $R_p$ values were obtained from the measurements with sinapinic acid, compared with gentisic acid, which confirms the results of potentiodynamic polarization measurements.

### *3.2. Impedance measurements (EIS)*

In order to obtain a physical image of the systems observed and explain all processes at the Al alloy / solution phase boundary, impedance measurements have been performed. The measurements were carried out in a quiescent NaCl solution without and with the addition of different concentration of sinapinic and gentisic acid at 20 °C. The examination results are shown in Figures 6 and 7 in the Nyquist and Bode diagrams.

As can be seen two loops were observed in Nyquist diagram for Al-0.8Mg electrode in pure NaCl solution: the capacitive loop at high frequencies and inductive time loop at low frequency values. The high frequency capacitive loop could be assigned to the relaxation process in the natural oxide film and its dielectric properties, while the inductive behavior is probably caused by relaxation processes involving adsorbed species formed due to local dissolution at the oxide|electrolyte phase boundary, which determines the Faraday processes of the system examined [35-39].

In the Bode plots three distinctive segments can be observed. At high frequencies (f > 10 kHz) the data are dominated by electrolyte resistance. In the medium frequency region the slope of the log |Z| vs. log f curve close to -1 and the phase angle approaching $80^o$ determined the capacitive behaviour of the system. At the lowest frequencies, the shape of diagram pointed out on inductive behaviour of the system examined.

The obtained spectra show that the impedance changes rapidly with the inhibitor concentration (sinapinic and gentisic acids). The changes are observed through abrupt growth of diameter and size of capacitive semicircle and increases of overall system impedance, which indicating that the electrode surface gets more protection. Furthermore, at sinapinic acid concentrations $\geq 1 \times 10^{-5}$ mol $dm^{-3}$ and gentisic acid concentrations $\geq 5 \times 10^{-5}$ mol $dm^{-3}$ the inductive loop in the impedance diagram completely disappears pointed out on physical blocking of the alloy surface (formation of a thicker protective film) and prevention of local corrosion.

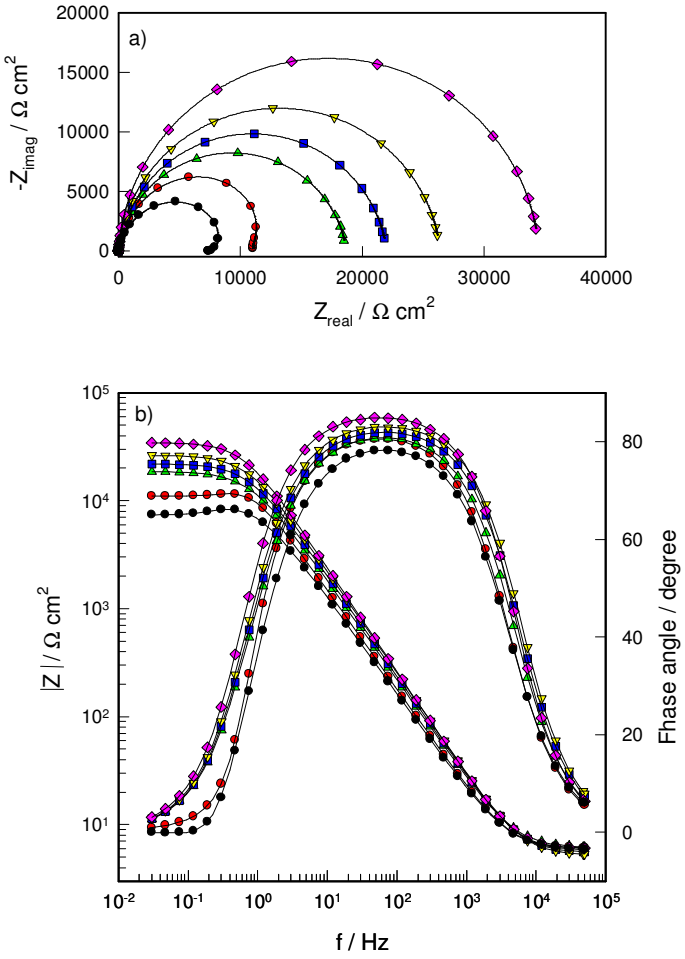


**Figure 6.** The Nyquist (a) and Bode (b) plots of the Al-0.8Mg alloy in a 0.5 mol dm$^{-3}$ NaCl solution at open circuit potential without (●) and in the presence of sinapinic acid in concentrations 1×10$^{-6}$ (●), 1×10$^{-5}$ (▲), 5×10$^{-5}$ (■), 1×10$^{-4}$ (▼) and 5×10$^{-4}$ mol dm$^{-3}$ (♦).

The capacitive properties of system considered in the presence of the phenolic acids are attributable to the dielectric properties of the surface (metal-oxide-inhibitor) adsorption layer.
The impedance spectra for the Nyquist plots were analyzed by fitting to the equivalent circuit models shown in Fig. 8.

The equivalent circuit marked with a) was found to fit the experimental data obtained in the NaCl solutions without, and with the addition of sinapinic acid in concentration 1×10$^{-6}$ mol dm$^{-3}$, and gentisic acid in concentration 1×10$^{-5}$ mol dm$^{-3}$. It consists of a CPE (substituting for capacity in the equivalent circuit n ≈ 1 and Q ≈ C) in parallel to the series resistors $R_1$ and $R_2$ and an inductance L in parallel to $R_2$. $R_{el}$ corresponds to the electrolyte resistance and it was found to be of order 5 Ω cm$^{-2}$. The equivalent circuit marked b) is used for modeling the experimental results for measurements in NaCl solution with higher concentration of sinapinic and gentisic acids. It consists of a parallel RQ combination connected in series with the electrolyte resistance.

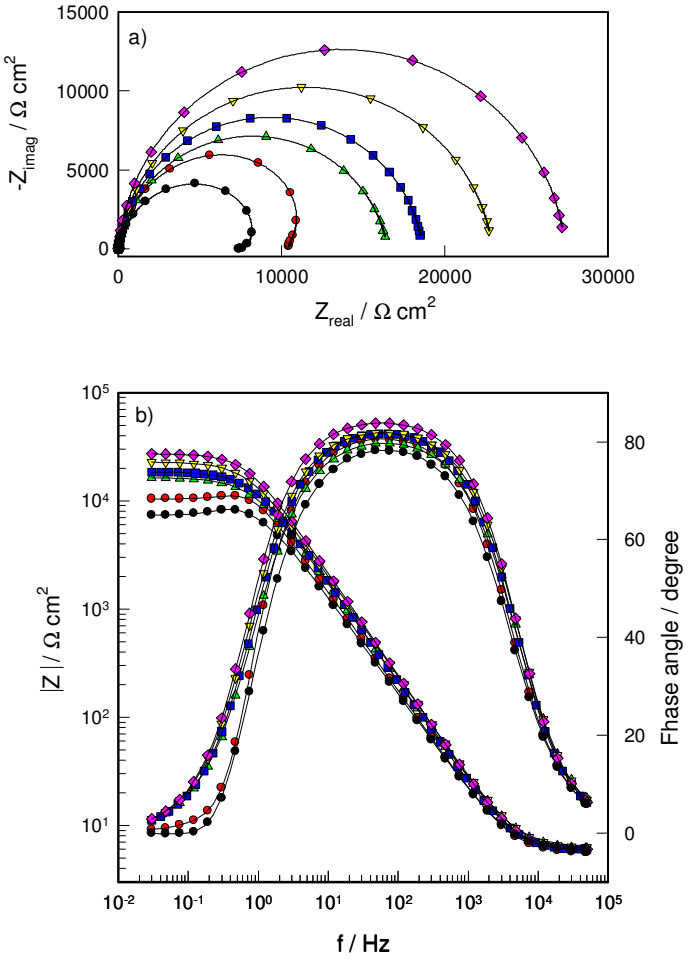


**Figure 7.** The Nyquist (a) and Bode (b) plots of the Al-0.8Mg alloy in a 0.5 mol dm$^{-3}$ NaCl solution at open circuit potential without (●) and in the presence of gentisic acid in concentrations 1×10$^{-5}$ (●), 5×10$^{-5}$ (▲), 1×10$^{-4}$ (■), 5×10$^{-4}$ (▼) and 1×10$^{-3}$ mol dm$^{-3}$ (♦).

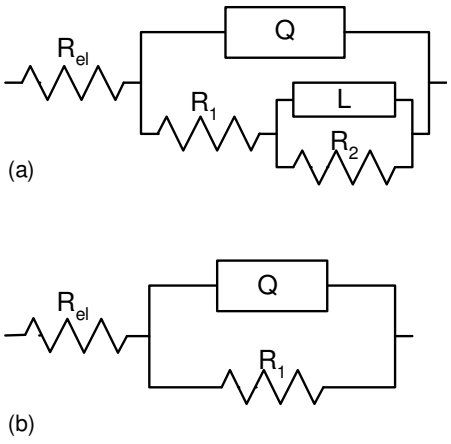


**Figure 8.** Equivalent circuits for modelling impedance data of the Al-0.8Mg alloy.

The use of CPE type impedance has been extensively described in the literature for this type of study.

Its impedance, $Z_{CPE}$, is described by expression:

$$Z_{CPE} = \frac{1}{Q(j\omega)^n} \quad (5)$$

where the constant Q accounts for a combination of properties related to both the surface and the electroactive species; $j\omega$ is the complex variable for sinusoidal perturbation with $\omega = 2\pi f$. Exponent n in Equation 5 for CPE impedance provides information about the degree of non-ideality in capacitive behavior. Its value makes it possible to differentiate between the behavior of CPE ($n < 1$) and that of an ideal capacitor ($n = 1$).

The calculated equivalent circuits parameters for Al alloy in chloride solution containing different concentrations of phenolic acids are presented in Table 3. The parameters Q, n, $R_1$, $R_2$ and L were evaluated using simple least square fitting procedure, and shown in the Table 3.

**Table 3.** Impedance parameters for the Al-0.8Mg alloy in 0.5 mol $dm^{-3}$ NaCl solution in the absence and in the presence of different concentrations of sinapinic acid and gentisic acid

| c (mol $dm^{-3}$) | $Q_1 \times 10^6$ ($\Omega^{-1}$ $s^n$ $cm^{-2}$) | $n_1$ | $R_1$ (k$\Omega$ $cm^2$) | L (kH $cm^{-2}$) | $R_2$ (k$\Omega$ $cm^2$) |
|---|---|---|---|---|---|
| sinapinic acid | | | | | |
| 0 | 18.58 | 0.90 | 7.36 | 1.21 | 2.49 |
| $1\times10^{-6}$ | 14.79 | 0.92 | 11.08 | 1.08 | 4.06 |
| $1\times10^{-5}$ | 12.11 | 0.92 | 18.68 | | |
| $5\times10^{-5}$ | 10.53 | 0.93 | 21.97 | | |
| $1\times10^{-4}$ | 9.16 | 0.94 | 26.37 | | |
| $5\times10^{-4}$ | 7.87 | 0.96 | 34.48 | | |
| gentisic acid | | | | | |
| $1\times10^{-5}$ | 15.21 | 0.92 | 10.46 | 1.16 | 3.87 |
| $5\times10^{-5}$ | 13.18 | 0.91 | 16.46 | | |
| $1\times10^{-4}$ | 11.85 | 0.93 | 18.62 | | |
| $5\times10^{-4}$ | 10.52 | 0.93 | 22.88 | | |
| $1\times10^{-3}$ | 9.07 | 0.95 | 27.35 | | |

The results obtained indicate that the increase in phenolic acids concentration leads to the increase the value of resistance $R_1$ (from 11.08 to 34.48 k$\Omega$ $cm^2$ for sinapic acid and from 10.46 to 27.35 k$\Omega$ $cm^2$ for gentisic acid) and the decrease of capacity of surface layer, Q. This direction of change is attributed to the increase of protective properties of the adsorbed layer at the surface of the electrode.

Furthermore, according to the plate capacitor model, the oxide film capacity, C, is inversely proportional to its thickness, d (according $C = \varepsilon_o\varepsilon/d$; $\varepsilon_o$ is the permittivity of vacuum, $\varepsilon$ is the relative permittivity of the film). Hence, the reduction of Q with the increase inhibitor concentration matches the corresponding increase of the thickness of the surface layer, which additionally indicated on increase of protective properties of the surface layer.

### *3.3. Adsorption behavior*

The interactions between the investigated inhibitors and the Al-0.8Mg alloy surface can be examined by the adsorption isotherms. The degree of surface coverage values for various concentrations of the inhibitors in 0.5 mol $dm^{-3}$ NaCl solution have been evaluated from the polarization measurements. Suitable adsorption isotherm was obtained, using these calculated values.

The linear relationships of ln Θ versus ln c, depicted in Fig. 9, suggest that the adsorption of sinapinic and gentisic acid on the Al-0.8Mg alloy surface obeyed the Freundlich adsorption isotherm.

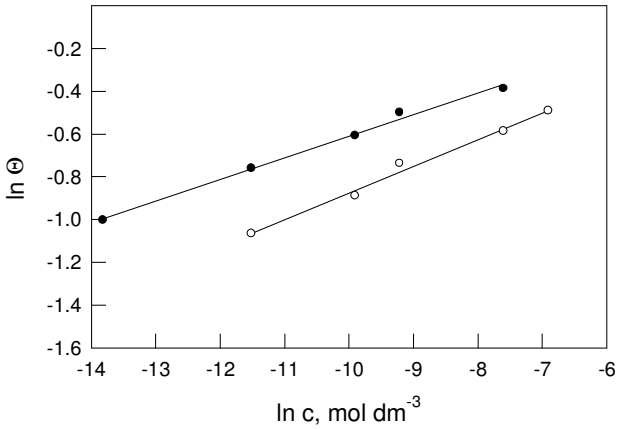


**Figure 9.** Adsorption isotherm for the sinapinic (●) and gentisic acid (○).

According to this isotherm, the surface coverage Θ is related to the equilibrium adsorption constant K and the concentration c via:

$$\Theta = Kc^n \tag{6}$$

where $0 < n < 1$, or

$$\ln\Theta = \ln K + n\ln c \tag{7}$$

The equilibrium constant of adsorption is related to the free energy of adsorption $\Delta G^o_{ads}$ by:

$$K = \frac{1}{55.5}\exp\left(-\frac{\Delta G^o_{ads}}{RT}\right) \tag{8}$$

The value of 55.5 is the concentration of water in the solution in mol $dm^{-3}$, R is the gas constant and T is the absolute temperature. Table 4 lists the thermodynamic data obtained from the adsorption isotherms.

**Table 4.** Adsorption equilibrium constant and standard free adsorption energy for the Al-0.8Mg alloy in 0.5 mol $dm^{-3}$ NaCl solution in the presence of sinapinic and gentisic acid

| | K ($dm^3$ $mol^{-1}$) | $\Delta G^o_{ads}$ (kJ $mol^{-1}$) |
|---|---|---|
| sinapinic acid | 1.49 | -10.755 |
| gentisic acid | 1.44 | -10.684 |

The negative values of $\Delta G^o_{ads}$ indicate that the adsorption process proceeds spontaneously. Values of $\Delta G^o_{ads}$ around -20 kJ $mol^{-1}$ or lower are consistent with the electrostatic interactions between organic molecules and charged metal surface (physisorption), while those around -40 kJ $mol^{-1}$ or higher involve charge sharing or transfer from the organic molecules to the metal surface (chemisorption) [8,40]. The numerical values of free energies of adsorption indicate physical adsorption of phenolic acids on the surface of the Al-0.8Mg alloy.

Physical adsorption developing is due to the electrostatic attraction between the inhibiting ions or dipoles and the electrical charged surface of the metal [41]. As the forces in electrostatic adsorption are weak, increasing in electrode rotation rate probably leads to smaller adsorption or even to desorption of adsorbed inhibitors from electrode surface. This is the reason for lowering the values of inhibition efficiency with increasing the electrode rotation rate.

This work presents results of corrosion inhibition of Al-0.8Mg alloys with two different phenolic acids, sinapinic and gentisic acid. Both acids showed similar behavior, they act as cathodic corrosion inhibitors, which physisorbed on the surface of investigated aluminium alloy, but there are differences in the values of surface coverage and inhibition efficiency. The origin of this differences lied on different chemical structure of these acids. Sinapinic acid belongs to the group of hydroxycinnamic acids while gentisic acid is hydroxybenzoic acid derivate. Sinapinic acid has chemical structure of an aromatic ring, two metoxy groups, one hydroxyl group and one carboxyl group. Gentisic acid has chemical structure of an aromatic nucleus, two hydroxyl groups and one carboxyl group. The literature indicates that organic compounds that contain hydroxyl or carboxyl groups may form complexes with metallic cations [4,42-44]. Results of some investigations showed that phenolic acids have ability to form complexes with different metal cations [45-47]. The presence of metoxy groups has strong influence on chelating property of phenolic acids [47]. The inhibitory action of investigated phenolic acids could be explained by the formation of complex molecules with aluminium ions and then precipitation of these complexes on aluminium alloy surface in places where oxide film was destroyed. Similar mechanism was proposed for corrosion inhibition of Al-2.5Mg alloy by (+)-catechine [17]. As sinapinic acid has bigger molecular size compared to the gentisic acid,

resulting complexes may cover higher electrode surface area, and this can be the one of the reason for higher values of inhibition efficiency for sinapinic acid.

## 4. CONCLUSIONS

1. Studying the corrosion inhibition effect and adsorption properties of two phenolic acids, sinapinic and gentisic acid on Al-0.8Mg alloy electrode in 0.5 mol $dm^{-3}$ NaCl solution it was found that both acids act as cathodic inhibitors for investigated alloy.

2. The inhibiting efficiency of the applied inhibitors is highest in a quiescent solution and at the lowest temperature examined and decreased with increasing electrode rotation rate and increasing electrolyte temperature, which indicate a weak interaction between the inhibitors molecules and the Al-0.8Mg alloy surface. The results of investigations have shown that sinapinic acid has better inhibiting characteristics then gentisic acid.

3. Adsorption of investigated phenolic acids on alloy surface obeys Freundlich adsorption isotherm. The calculated free energies of adsorption of sinapinic and gentisic acid on Al-0.8Mg alloy reveal physical adsorption of phenolic acids on the electrode surface.

4. The inhibitory action of investigated phenolic acids could be explained by the formation of complex molecules with aluminium ions and then precipitation of these complexes on aluminium alloy surface in places where oxide film was destroyed.

## References

1. C. Vargel, Corrosion of Aluminium, Oxford, Elsevier, 2004.
2. V. Guillaumin, and G. Mankowski, *Corros. Sci.*, 42 (2000) 105.
3. B. Davó, and J.J. Damborenea, *Electrochim. Acta*, 49 (2004) 4957.
4. L. Garrigues, N. Pebere, and F. Dabosi, *Electrochim. Acta*, 41 (1996) 1209.
5. M. Kliškić, J. Radošević, and S. Gudić, *J. Appl. Electrochem.*, 27 (1997) 947.
6. M. Bethencourt, F.J. Botana, J.J. Calvino, M. Marcos, and M.A. Rodriguez-Chacón, *Corros. Sci.*, 40 (1998) 1803.
7. W.A. Badawy, F.M. Al-Kharafi, and A.S. El-Azab, *Corros. Sci.*, 41 (1999) 709.
8. Z. Grubač, R. Babić, and M. Metikoš-Huković, *J. Appl. Electrochem.*, 32 (2002) 431.
9. G.Y. Elewady, I.A. El-Said and A.S. Fouda, *Int. J. Electrochem. Sci.,* 3 (2008) 177.
10. G.Y. Elewady , I.A. El-Said and A.S. Fouda, *Int. J. Electrochem. Sci.*, 3 (2008) 644.
11. A.Y. El-Etre, *Corros. Sci.,* 43 (2001) 1031.
12. G. Bereket and A. Yurt, *Corros. Sci.*, 43 (2001) 1179.
13. G.O. Avwiri and F.O. Igho, *Mater. Lett*., 57 (2003) 3705.
14. B. Müller, *Corros. Sci*., 46 (2004), 159.
15. I.B. Obot, N.O. Obi-Egbedi, *Int. J. Electrochem. Sci.*, 4 (2009) 1277.
16. A. Bouyanzer, B. Hammouti, L. Majidi, *Mater. Lett.*, 60 (2006) 2840.
17. M. Kliškić, J. Radošević, S. Gudić, V. Katalinić, *J. Appl. Electrochem*., 30 (2000) 823.
18. E.E. Oguzie, *Corros. Sci.*, 49 (2007) 1527.
19. L. Vrsalović, M. Kliškić, J. Radošević and S. Gudić, *J. Apply Electrochem.*, 35 (2005) 1059.
20. J. Radošević, M. Kliškić and A. Višekruna, *Kem. Ind.*, 50 (2001) 537.

21. M. Kliškić, J. Radošević and S. Gudić, Proceedings of the 9th European Symposium on Corrosion Inhibitors, Ann. Univ. Ferrara, N.S., Sez, V. Suppl. N. 11, 2000, p. 127.
22. L. Vrsalović, M. Kliškić, J. Radošević and S. Gudić, *J. Apply. Electrochem*., 37 (2007) 325.
23. E.M. Marinova and N.V. Yanishlieva, *Food Chem*., 81 (2003) 189.
24. J. Pokorny, N. Yanishlieva and M. Gordon, Antioxidants in food, Woodhead Publishing Limited, Cambridge England, 2001.
25. M.S. Barber, V.S. McConnell and B.S. DeCaux, *Phytochemistry*, 54 (2000) 53.
26. M.A. Fernandez, M.D. Garcia and M.T. Saenz, *J. Ethnopharmacol*., 53 (1996) 11.
27. B.G. Cubley, Chemical Inhibitors for Corrosion Control, The Royal Society of Chemistry, 1990.
28. K. Shimizu, G.M. Brown, K. Kobayashi, P. Skeldon, G.E. Thompson, G.C. Wood, *Corros. Sci.,* 40 (1998) 1049.
29. R. Wen-da, L. Jin-feng, Z. Zi-qiao, C. Wen-jing, *Trans. Nonferrous. Met. Soc. China,* 17 (2007) 727.
30. J. R. Flores, H. Terryn, O. Steenhaut, J.H. de Wit, Abs. 502, 204th Meeting, Electrochem. Soc. Inc., 2003.
31. R.H. Jones, J.S. Vetrano and C.F. Windisch, *Corrosion,* 60 (2004) 1144.
32. J. Campbell and R.A. Harding, TALAT Lecture 3208, European Aluminium Association, 1994.
33. Lj.M. Vračar and D.M. Dražić, *Corros Sci*., 44 (2002) 1669.
34. A. Popova, E. Sokolova, S. Raicheva and M. Christov, *Corros Sci*., 45 (2003) 33.
35. D.D. Macdonald, *Electrochim. Acta*, 35 (1990) 1509.
36. F. Mansfeld, S. Lin, S. Kim and H. Shih, *Werkst. Korros*., 39 (1988) 487.
37. J.B. Bessone, D.R. Salinas, C.E. Mayer, M. Ebert and W.J. Lorenz, *Electrochim. Acta*, 37 (1992) 2283.
38. H.J.W. Lendernik, M.V.D. Linden and J.H.W. De Wit, *Electrochim. Acta*, 38 (1993) 1989.
39. A. Frichet, P. Gimenez and M. Keddam, *Electrochim. Acta*, 38 (1993) 1957.
40. H. Keles, M. Keles, I. Dehri and O. Serindag, *Mater. Chem. Phys*., 112 (2008) 173.
41. V.S. Sastri, Corrosion Inhibitors Principles and Applications, John Wiley & Sons, West Sussex, England, 2001.
42. B. Muller, *Corros Sci.*, 46 (2004) 159.
43. J. Mabrour, M. Akssira, M. Azzi, M. Zertoubi, N. Saib, A. Messaoudi, A. Albizane and S. Tahiri, *Corros Sci*., 46 (2004) 1833.
44. L. Valek, S. Martinez, M. Serdar and I. Stipanović, *Chem Biochem Eng Q.,* 21 (2007) 65.
45. S. Giroux, S. Aury, P. Rubini, S. Parant, J.-R. Desmurs and M. Dury, *Polyhedron*, 23 (2004) 2393.
46. F. Borges, C. Guimaraes, J.L.F.C. Lima, I. Pinto and S. Reis, *Talanta*, 66 (2005) 670.
47. K. Zhou, J.-J. Yin and L.L. Yu, *Food Chem.*, 95 (2006) 446.